We are IntechOpen, the world's leading publisher of Open Access books Built by scientists, for scientists

6,900
Open access books available

185,000
International authors and editors

200M
Downloads

Our authors are among the

154
Countries delivered to

TOP 1%
most cited scientists

12.2%
Contributors from top 500 universities



WEB OF SCIENCE™

Selection of our books indexed in the Book Citation Index in Web of Science™ Core Collection (BKCI)

Interested in publishing with us?
Contact book.department@intechopen.com

Numbers displayed above are based on latest data collected.
For more information visit www.intechopen.com



Chapter 6

Analysis of the Spatial Separation Effects of Thorium/Uranium Fuels in Block-Type HTRs

Ming Ding and Jie Huang

Additional information is available at the end of the chapter

http://dx.doi.org/10.5772/intechopen.68671

Abstract

With the rapid development of nuclear energy, thorium has been gaining attention because of its abundant reserves and excellent physical properties. Compared with light-water reactors, block-type high temperature gas cooled reactors (HTRs) are a better choice for thorium-based fuel for higher burnup and harder neutron spectrum. When using thorium in block-type HTRs, the composition and spatial distribution of thorium/uranium fuels are two determined factors of nuclear performance. Four spatial separation levels of thorium/uranium fuels, no separation level, TRISO level, channel level, and block level, are defined for the block-type thorium-fueled HTRs. A two-step calculation scheme was used to obtain the neutronic performance, including the initial inventory of U-235, effective multiplication factor, and average conversion ratio. Based on these data, the fuel cycle cost of different spatial separation levels can be calculated by the levelized lifetime cost method as a function of thorium content. The fuel cycle cost changes with the same trend as the initial inventory of U-235 in the reactor cores because the latter determines 70% of the total cost. When the thorium content is constant, the initial inventory of U-235 decreases with the increase of the spatial separation level because spatial self-shielding effect is strengthened by the latter.

Keywords: spatial separation effects, Th/U MOX, seed-and-blanket concept, whole assembly seed-and-blanket concept, block-type HTRs, fuel cycle cost analysis

INTECH
open science | open minds

© 2017 The Author(s). Licensee InTech. This chapter is distributed under the terms of the Creative Commons Attribution License (http://creativecommons.org/licenses/by/3.0), which permits unrestricted use, distribution, and reproduction in any medium, provided the original work is properly cited. CC BY

1. Introduction

During the mid-1950s to the mid-1970s, some different types of Th/U MOX fuels, for example $(Th,U)O_2$ or $(Th,U)C_2$, were tested and used as fuels in high-temperature gas-cooled reactors (HTRs), like AVR and THTR in Germany [1] and Fort St. Vrain in the USA [2]. Three main reasons inspired them to demonstrate Th-U fuel cycle at that time. First, compared with kwon uranium, thorium is three times more abundant in nature. Second, Th-232 has an attractive potential for breeding to fissile U-233 efficiently in thermal neutron spectrum. U-233 is also considered as the best compared with other two common fissile isotopes, U-235 and Pu-239, in epithermal or thermal spectrum from neutronic point of view because the number of fission neutrons per neutron absorbed is 10–20% higher than that of U-235 and Pu-239. Finally, uranium resources were believed to be insufficient to support the development of nuclear industries on a large scale at the early period of nuclear energy development.

Besides HTRs, thorium has been an interesting nuclear fuel for various reactor applications [3], such as molten-salt reactors (MSRs) and water-cooled reactors.Especially, combined with molten-salt fuel in MSRs, thorium was used as a necessary composition of the "standard" fuel aiming to converse and even breed Th-232 to U-233 from the 1970s to mid-1980s. In past 20 years, the potential of thorium has been extended to radioactive waste management and plutonium incineration [4]. In this application, Th-232 is considered as a better fertile isotope than U-238 because of a larger net destruction of plutonium, when weapon-grade or reactor-grade plutonium is burned in various nuclear reactors. Furthermore, thorium-fueled reactors generate less long-lived radioactive wastes than uranium-fueled ones.

Combined with the commercial purpose and potential application scale, light-water reactors (LWRs) are a natural choice from the reactor point of view in recent years because of a large amount of LWRs all over the world. The seed-and-blanket (S&B) concept has been reexamined for LWR application by the MIT group [5, 6]. The concepts originate from S&B configuration and were developed for the advanced water breeder application (AWBA) program and tested in the light water breeder reactor (LWBR) at Shippingport from 1977 to 1982 [7]. Further work on thorium-fueled LWRs has been pursued by Radkowsky and Galperin [8]. The MIT group proposed the micro-heterogeneous fuel assemblies and the whole assembly seed-and-blanket (WASB) concept. Moreover, compared with the past research, the recent MIT work is all based on low-enriched uranium for proliferation resistance.

Because of the burnup limit of LWRs (usually 50 GWd/tHM), some research showed that the potential of thorium is limited in LWRs, and HTRs are a better choice for thorium-based fuel for higher burnup and harder neutron spectrum. Recently, the concept of S&B fuel blockshas been introducedto the U-battery [9], a small long-life HTR, and a commercial-level GT-MHR [10], as well as advanced high-temperature reactors (AHTRs) [11] with low-pressure liquid-salt (Flibe) as coolant, which enables the design of a high-power (e.g., 2400–4000 MWth), high-temperature (850–950°C) reactor with fully passive safety capability and the economic production of electricity orhydrogen.

The past studies have shown the distribution of thorium and uranium fuels in space is a very important factor for the performance of thorium-fueled reactors and have proposed some

http://dx.doi.org/10.5772/intechopen.68671

interesting concepts of S&B and WASB. Actually, the different concepts represent different separation levels of thorium/uranium fuels in space. The chapter tries to systematically analyze the spatial separation effects of thorium/uranium fuels on the nuclear performance of block-type HTRs and to quantitatively evaluate the difference by fuel cycle cost. The second section will describe the reactor, fuel block, and the calculation models, including the transport calculation model with burnup and fuel cycle cost model. The third section will present the calculation results of four different spatial separation levels and discuss the difference among them. The final section will conclude the chapter.

2. Block-type HTRs and calculation methodologies

2.1. Block-type HTRs and spatial separation levels

2.1.1. Block-type HTRs

Modular block-type HTRs [12] are one kind of inherently safe reactors, which passively remove decay heat by natural convection, conduction, and radiation from the reactor core and keep the fuel intact. As mentioned in Section 1, the block-type HTRs are a better choice for thorium-based fuel for higher burnup and harder neutron spectrum. Moreover, an advantage of block-type HTRs over pebble-bed HTRs is that the former provides multi-level and fixed spatial distribution of thorium/uranium fuels in the reactor cores.The reactor core of the block-type HTRs investigated, as shown in **Figure 1(a)**, is comprised of an annular fuel zone, inner reflectors, and outer reflectors. The annular fuel zone is comprised of 1980 fuel blocks, as shown in **Figure 1(b)**. The fuel blocks are stacked firmly against each other in columns that form an annulus between an inner and an outer reflector, both of which consist of rings of unfueled graphite blocks. The annular core configuration ensures higher thermal power and inherent safety under most accidents and transient conditions. Each fuel block includes 210 fuel channels, 108 coolant channels, and 6 fixed burnable poison channels which are filled with

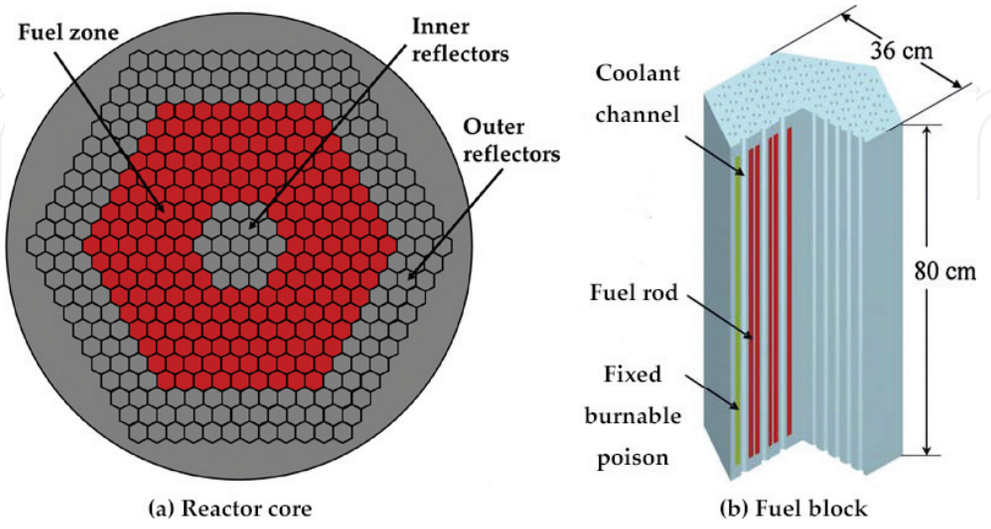


Figure 1. Thorium-fueled HTR and fuel block, (a) Reactor core and (b) Fuel block. Does the query aim to use second style for the book?

graphite in the flowing calculations.The cylindrical fuel compacts are stacked inside channels drilled into hexagonal graphite blocks. Other geometrical parameters ofthe fuel blocks are listed in **Table 1**.

The most prominent feature of the block-type HTRs is use of tristructural-isotropic (TRISO) particles, which contain five layers from inside to outside: fuel kernel, porous carbon buffer, inner pyrolytic carbon (IPyC), silicon carbide (SiC), and outer pyrolytic carbon (OPyC). The porous carbon buffer layer is provided to protect the dense PyC from fission recoil damage and to provide void volume to limit the fission gas pressure. The dense PyC has good irradiation stability and capability to remain intact to perform fission production retention under severe exposure conditions. Sandwiched between the two PyC layers, the SiC layer provides metallic fission production retention and mechanical strength. TRISO fuel particles are blended and bonded together with a graphite matrix to form fuel compacts. **Figure 2** illustrates how the TRISO particles are packaged into the annular core.

2.1.2. Definition of multiscale spatial separation

When using thorium in HTRs, two important factors influence nuclear performance. One is the thorium content (the mass ratio of Th-232 to all heavy metal isotopes), meaning the mixed proportion of thorium and uranium. The other is the spatial separation level of thorium and uranium, meaning how thorium and uranium are to be mixed. According to the level of spatial separation, four levels are in a block-type HTR: (1) No separation (Th/U MOX level): with Th/U MOX fuel, the thorium and uranium are mixed in each fuel kernel as a form of $(Th,U)O_2$, as shown in **Figure 2(a)**. Thorium and uranium do not separate in the macrolevel, (2) TRISO-level separation (SBT level): UO_2 and ThO_2 are made into different TRISO fuel particles (UO_2 TRISO and ThO_2 TRISO) separately, but the two kinds of TRISO fuel particles are mixed into the same fuel compact, as shown in **Figure 2(b)**, (3) Channel-level separation (SBU level): each fuel channel has only one kind of fuel compacts (UO_2 fuel compacts or ThO_2 fuel compacts), but a fuel block has both UO_2 fuel channels and ThO_2 fuel channels, as shown in **Figure 2(c)**, and (4) Block-level separation (WASB level): each fuel block only has a kind of fuel (UO_2 or ThO_2), but the core has both UO_2 fuel blocks and ThO_2 fuel blocks, as shown in **Figure 2(d)**.

2.2. Calculation and evaluation methods

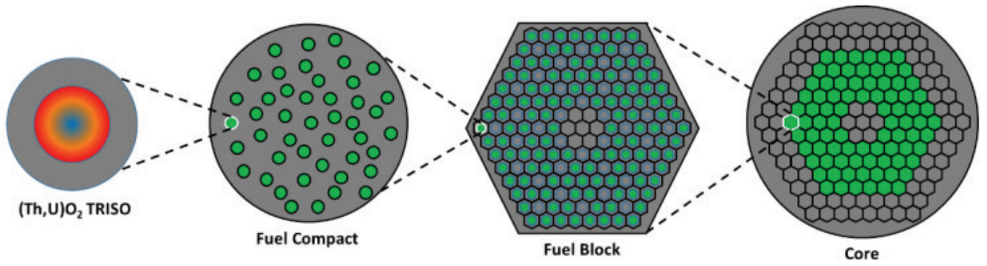
2.2.1. Neutronic calculation method

To only analyze the influence of spatial separation, the other parameters are kept the same including the fuel block geometry, as listed in **Table 1**, and the fuel shuffling scheme, as shown in **Figure 3**. A detailed full-core 3D transport calculation in one step will require significant

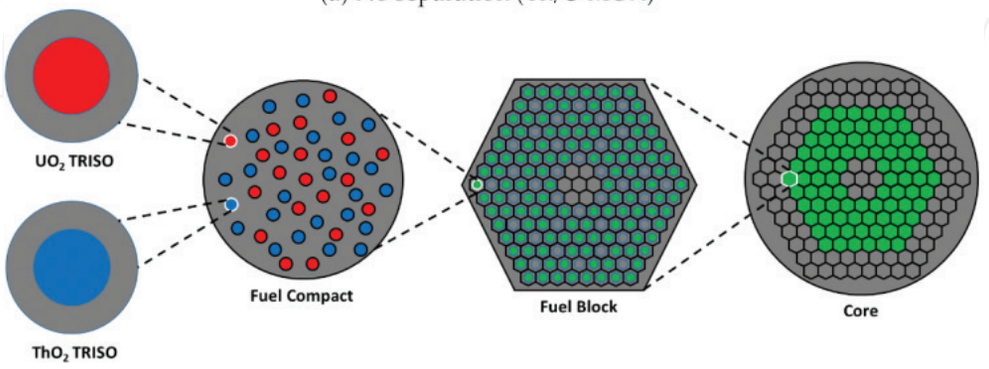
Parameters	Width across flat [cm]	Height of block [cm]	Diameter/ number of fuel channels [cm/−]	Diameter/number of coolant channels [cm/−]	Diameter of kernels [μm]	Thickness of TRISO layers [μm]	Density of TRISO layers [g/cm^3]
Values	36	79.3	1.27/210	1.588/102, 1.27/6	500	100/35/35/40	1.05/1.9/3.2/ 1.9

Table 1. Basic geometrical parameters of fuel blocks in the HTR.

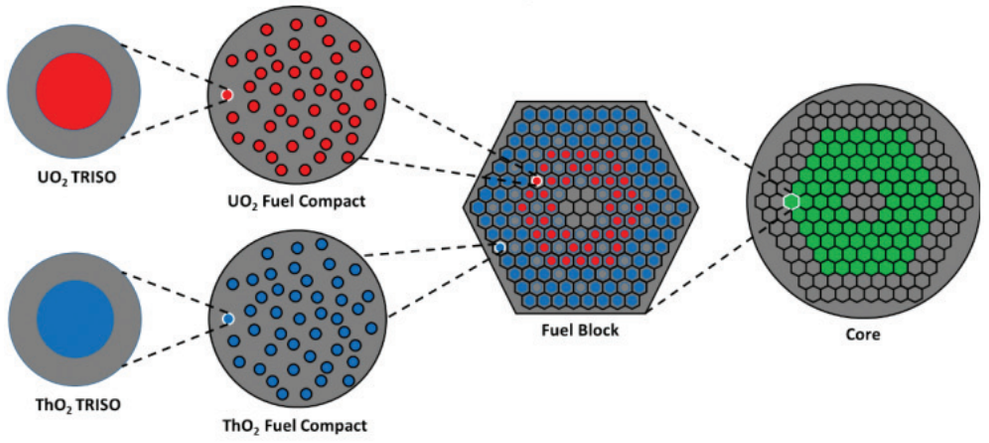
http://dx.doi.org/10.5772/intechopen.68671



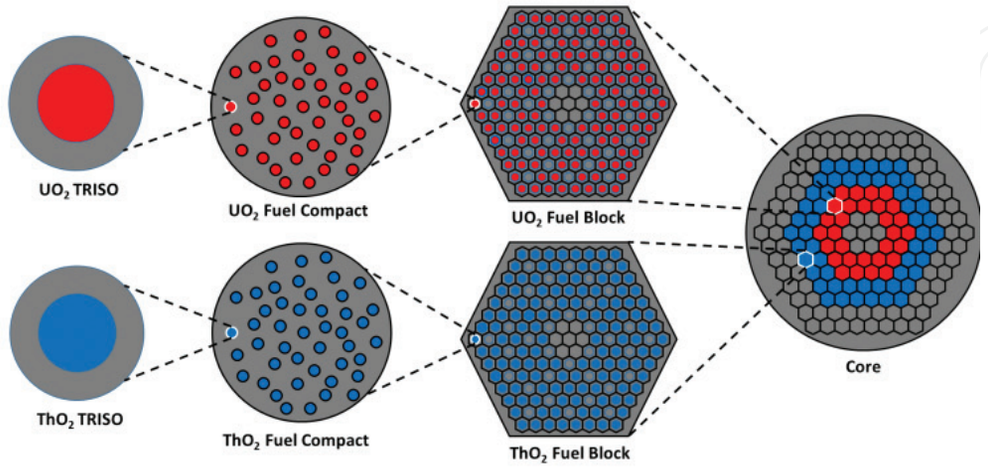
(a) No separation (Th/U MOX)



(b) TRISO-level separation (SBT)



(c) Channel-level separation (SBU)



(d) Block-level separation (WASB)

Figure 2. Four levels of spatial separation of thorium/uranium in block-type HTRs.

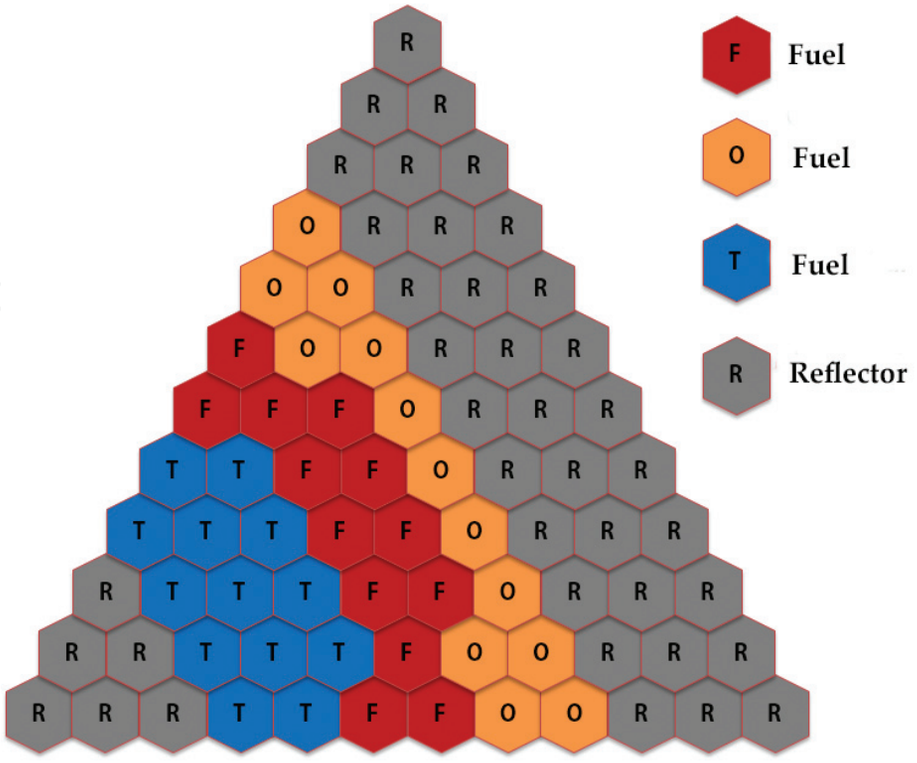


Figure 3. Reactor core calculation model for 1/6th core.

memory and a central processing unit (CPU) time as utilities in producing calculations or even in laboratories for design purposes. Therefore, a two-step calculation scheme is typical: (1) a detailed calculation at the assembly level with reflective boundary conditions, which gives homogenized cross-sections for the assemblies, condensed to a certain number of groups (lattice calculation step) and (2) a second calculation at the core level with homogenized properties in each assembly and usually small number of groups (full-core calculation step).

In this chapter, the traditional two-step calculation scheme is constructed based on the DRAGON V4 code system [13], as shown in **Figure 4**. An attractive feature of the DRAGON code is its ability to treat particle fuel in a graphite matrix in a full-assembly calculation. It provides the possibility to define a stochastic mixture of spherical micro-structures that can be distributed inside composite mixtures of the current macro-geometry using the Hebert double-heterogeneity model [14] or Sanchez-Pogroming double-heterogeneity model [15].

In step (a) in **Figure 4**, a 2D fuel block is modeled including the structure of the TRISO particle. The method of characteristics (MOC) and 295-group cross-section library (http://www.polymtl.ca/merlin/libraries.htm) are used to solve the transport equation. Then, the energy groups of the cross-sections are condensed to 26 groups during the homogenization of the fuel block. In step (b), a 1D annular core is modeled, comprising a homogenized fuel zone and two reflector zones. The homogenized cross-sections of the fuel block generated in step (a) are used for the fuel zone in this step, and the cross-sections of the graphite generated in step (a) are used for the reflectors of the 1D reactor model. The 1D transport calculations are executed by the discrete ordinate (S_N) method. Only the reflectors are homogenized to generate the

http://dx.doi.org/10.5772/intechopen.68671

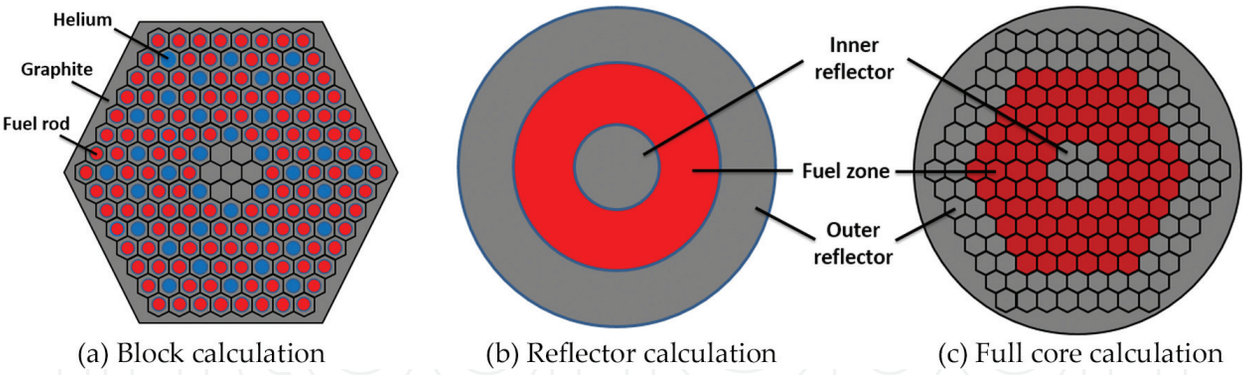


Figure 4. A schematic diagram of the two-step calculation scheme.

cross-sections of the reflector for the following full-core calculations. In step (c), the 2D full-core calculations are executed by the interface current (IC) method. The cross-sections of fuel blocks in this step come from the step (a), while the cross-sections of reflectors come from step (b).

2.2.2. Fuel cost analysis model

An evaluation criterion must be in the comparison of different spatial separationlevels. Usually, the fuel cycle cost is one of the criteria. To make a fair comparison, the adoption of a standardized methodology for fuel cycle cost calculations is prerequisite. Therefore, the levelized lifetime cost methodology is used in this study. The levelized lifetime cost methodology was developed by the Organization for Economic Cooperation and Development (OECD) [16], which uses an internationally accepted investment appraisal methodology to analyze the fuel cycle cost.

The cash flow for fuel cycle material and services commences before the reactor starts to generate electricity and continues well after the reactor ceases operation. The exact timing of payments for natural uranium purchase, conversion, enrichment, fabrication, spent fuel storage, and disposal depends on the associated lead and lag times for the fuel cycle components. To calculate the overall fuel cycle cost, the magnitude of each component cost and the appropriate time that it occurs must be identified. Fuel quantities are obtained from reactor neutronic calculations as described in Section 2.2.1. These quantities of materials and services are adjusted to allow for process losses in the various component stages of the nuclear fuel cycle and then multiplied by the unit costs to obtain the component costs. Finally, the total fuel cycle cost is gotten by discounting these component costs to their present values in a specified base year (usually the commission date of reactor), as shown in **Figure 5**. The levelized lifetime cost methodology provides costs per unit of electricity generated which are the ratios of lifetime expenses to total expected output, expressed in terms of the present value equivalent. This method derives economic merits by comparing their respective average levelized lifetime costs.

The reactor data and fuel cycle cost data for the HTR are shown in **Tables 2** and **3**, respectively. **Table 2** gives the information about the reactor including the power, lifetime, cycle length, and back-end options. **Table 3** gives the unit price and lead or lag time for natural uranium

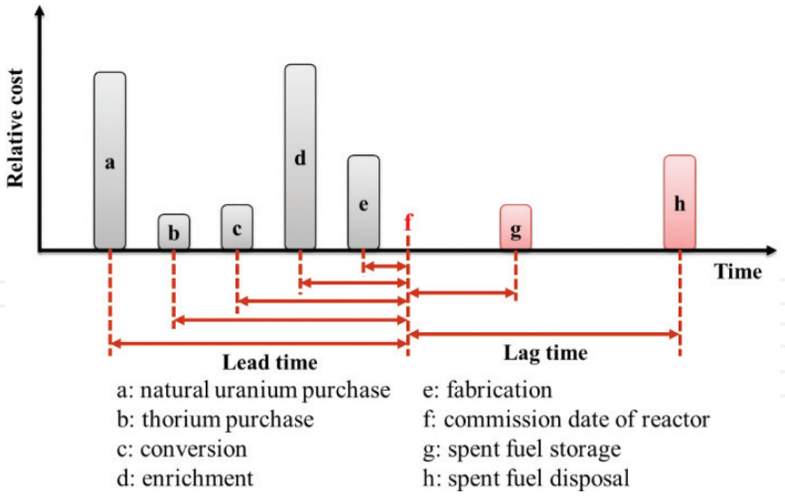


Figure 5. Time flow of nuclear fuel cycle cost with direct disposal option.

Items	Values
Thermal output	600 MWth
Electric output	240 MWe
Plant lifetime	60 years
Refueling cycle length	2 years
Load factor	90%
Back-end options	Direct disposal
Discount rate	8%

Table 2. Reactor operation data for the HTR.

Components	Prices	Lead or lag times
Natural uranium purchase	120.9 $/kg U	24 months
Thorium purchase	120.9 $/kg Th	24 months
Conversion	8.75 $/kg U	18 months
Enrichment	126.5 $/SWU	12 months
Fabrication	777 $/kg HM	6 months
Storage	230 $/kg HM	5 years
Disposal	610 $/kg HM	40 years

Table 3. Fuel cycle cost data for the HTR.

purchase, thorium purchase, conversion, and enrichment. The price of natural uranium, conversion, and enrichment is the average price of spot market from 2010 to 2015 (http://www.uxc.com/), respectively: 120.9 $/kg U, 8.75 $/kg U, and 126.5 $/SWU. The fabrication cost of 777 $/kg HM for HTR fuel blocks comes from the Oak Ridge National Laboratory (ORNL)'s

report [17]. Others are the same as the OECD's report [16]. Although different fuel separation levels would likely affect unit price related to fabrication and, in particular, storage, and disposal, their fraction in total fuel cycle cost is small, as mentioned in Section 3.4. Moreover, the sensitivity analysis shows that a ±50% variation of the price of fabrication, storage, or disposal will lead to a no-more-than ±5% variation of fuel cycle cost [18]. Thus, even if different fuel separation levels have a different price of fabrication, storage, and disposal, the analysis in this chapter is still valid.

3. Results and discussion

For real HTRs with multi-batch refueling and multi-block, both the spatial separation levels defined in Section 2 and refueling patterns influence the performance of fuel in the reactor core, so the latter is excluded by ideally adopting one-batch fixed-patternrefueling mode in order to focus on the spatial separation effect of the thorium/uranium fuel. Based on the one-batch fixed-pattern refueling mode, as shown in **Figure 3**, thorium and uranium in the different spatial separation levels with the same mass are loaded into the geometrically same reactor core and are discharged when the k_{eff} reaches the same specified value. The core performance difference is due to the spatial separation levels.

3.1. Configuration effects in one spatial separation level

In order to compare four different spatial separation levels in the core scale, the configurations or patterns of the thorium/uranium fuels in the channel-level separation and block-level separation are simply analyzedin this section because the former meets different configurationsor patterns in block scale and the latter does in core scale, as shown in **Figure 2**, and the configurations influence the performance of the reactor core. For the other two separation levels, that is no separation level and TRISO-level separation, the same the fuel blocks exist in the whole reactor core.

3.1.1. Spatial configuration effects in the channel-level separation

For the channel-level separation, the spatial configurations of thorium/uranium compacts in the fuel block are different even for the same thorium content because uranium and thorium compacts are located in different channels, that is, there are 2^{210} configurations theoretically. It is almost impossible to investigate all of them, but it is not necessary to do it because the performance is possibly similar for some similar configurations, and the comparison in the reactor core scale is of the main concern. Five typical configurations (SBU 1#–SBU 5#) are chosen and investigated for 46% of thorium content, as shown in **Figure 6**. The uranium fuel compacts are located in the central, middle, and outer regions of the fuel block, respectively, for the SBU 1#–SBU 3#, and are evenly located in the fuel block for the SBU 4# and SBU 5#. The uranium compacts are relatively concentrated in the former group of configurations and are relatively dispersed in the latter group of configurations. For other thorium content, the spatial separation of uranium/thorium compacts are located in the similar mode.

Figures 7 and **8** show the k_{eff} of the reactor core for 46 and 91% thorium contents, which are calculated based on the model described in Section 2.2. When the thorium content increases, the number of thorium compacts will increase and the number of uranium compacts will decrease. In order to maintain the same mass of U-235 in the fuel block or in the reactor core,

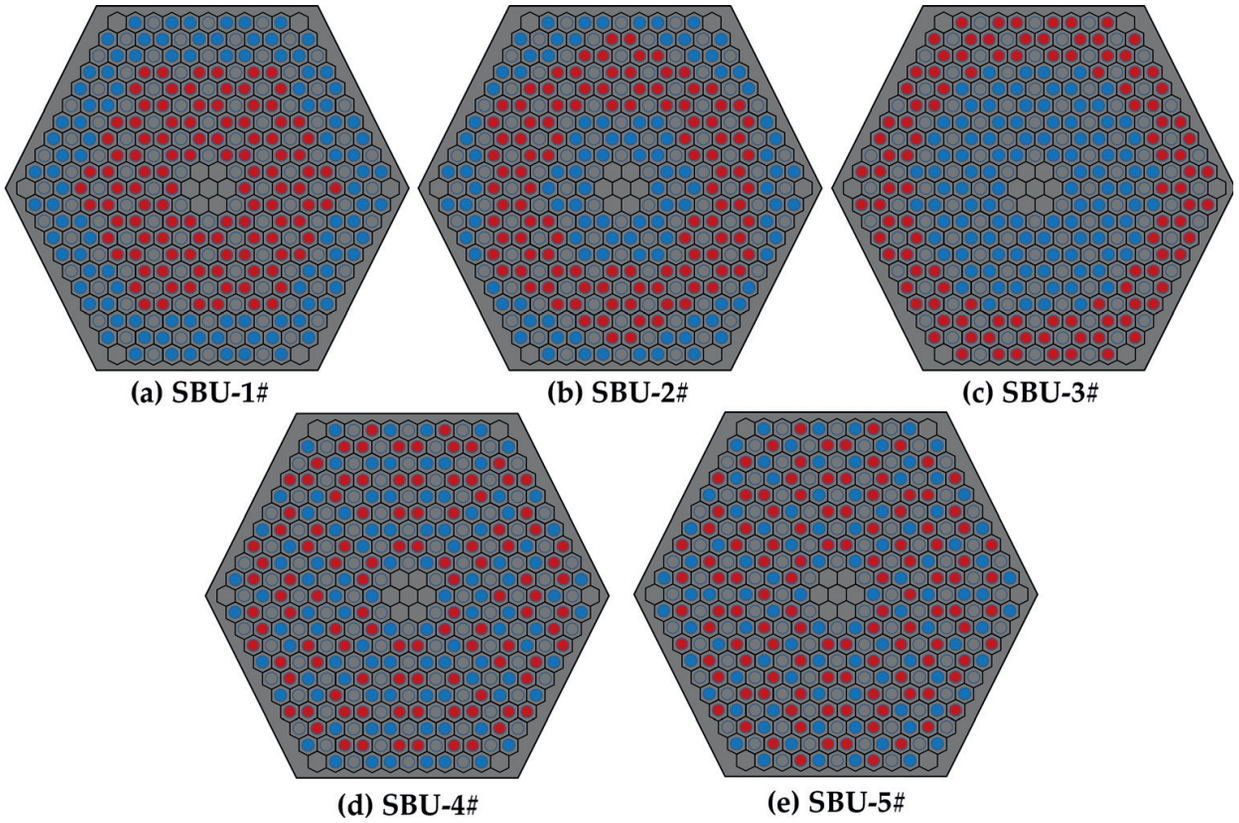


Figure 6. Five typical configurations of uranium/thorium fuels for 46% thorium content (red: uranium compacts, blue: Thorium compacts).

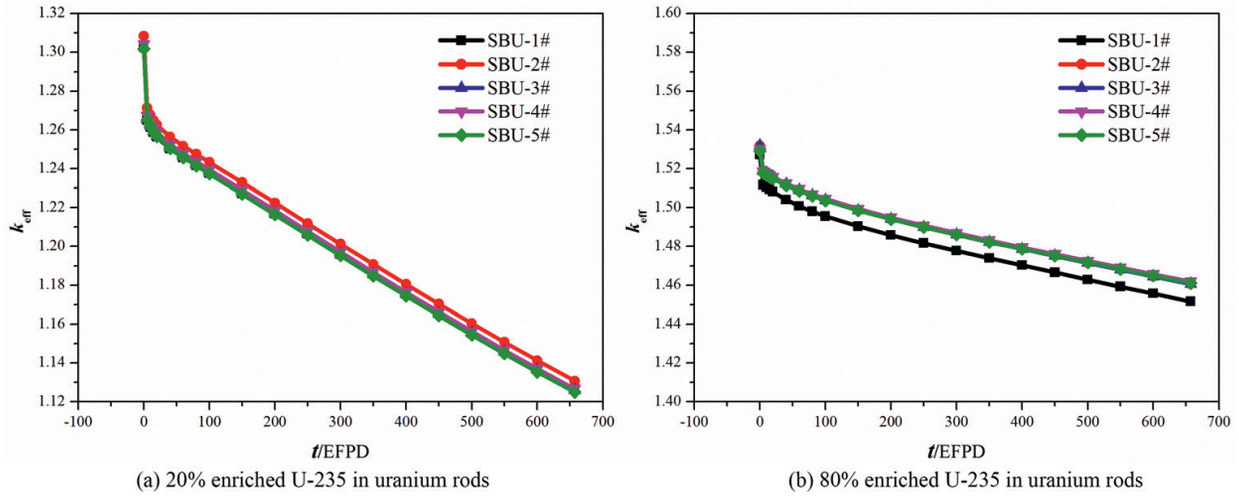
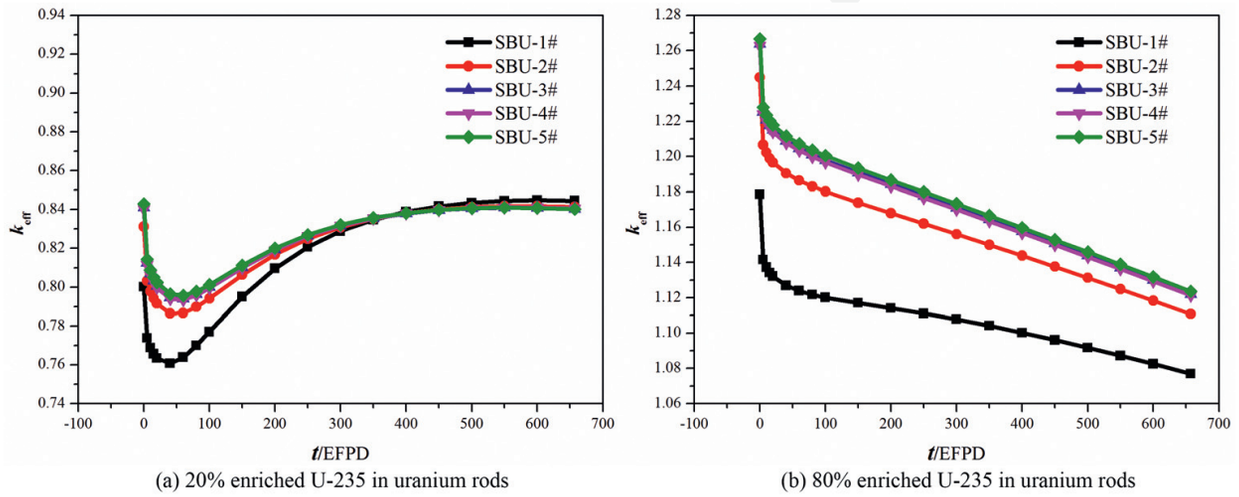


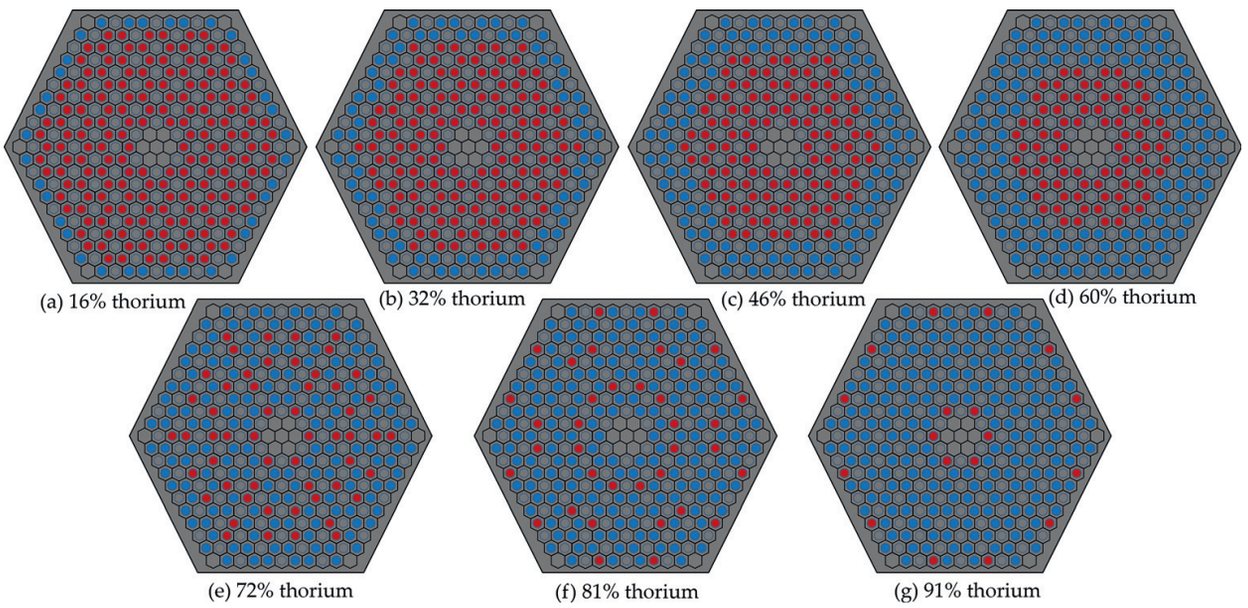
Figure 7. k_{eff} of five configurations for 46% thorium content.

the enrichment of U-235 has to be increased. For different thorium contents, when the enrichment of U-235 is less than 20%, the five different spatial configurations of thorium/uranium fuels achieve the similar k_{eff}. However, when the enrichment is higher than 20%, for example 80%, the k_{eff} of the five configurations is different obviously. Moreover, the k_{eff} of the SBU 4# and SBU 5# is always higher than the other three configurations, and the influence of the spatial configurations becomes important. In the channel-level separation, the dispersed uranium compacts are advantageous to transmute Th-232 to U-233 when the thorium content and, thus, the enrichment of U-235 are high. Based on the calculations and analysis, the suggested spatial configurations of thorium/uranium compacts in the fuel block are shown in **Figure 9** for the channel-level separation. The uranium compacts are concentrated in the



(a) 20% enriched U-235 in uranium rods (b) 80% enriched U-235 in uranium rods

Figure 8. k_{eff} of five configurations for 91% thorium content.



(a) 16% thorium (b) 32% thorium (c) 46% thorium (d) 60% thorium
(e) 72% thorium (f) 81% thorium (g) 91% thorium

Figure 9. Configurations of thorium/uranium compacts for channel-level separation (red: uranium compacts, blue: thorium compacts).

central region of the fuel block for low thorium content and are dispersed for high thorium content.

3.1.2. Spatial configuration effects in block-level separation

For the block-level separation, the spatial configurations of thorium/uranium fuel blocks in the reactor coremeet the same problem as the channel-level separation. The uranium and thorium fuel blocks located in different positions in the reactor core lead to different configurations, that is, there are 2^{198} configurationsof the fuel blocks theoretically. Based on the same analysis method as presented in Section 3.1.1, every five typical configurations (WASB 1#–WASB 5#) were chosen and investigated for different thorium content. The results show that the dispersed thorium fuel blocks are advantageous to transmute Th-232 to U-233 in the block-level separation. Based on the results, the suggested spatial configurations of thorium/uranium fuel blocks in the reactor core are shown in **Figure 10** for the block-level separation, which is chosen to be compared with other three separation levels.

3.2. Effective enrichment and initial inventory of U-235

As mentioned in Section 3.1, the highly-enriched U-235 possibly has to be used when the thorium content increases. Compared with thorium/uranium-fueled reactor, the uranium-fueled reactor only contains one fissile isotope, that is, U-235, and one fertile isotope, that is,

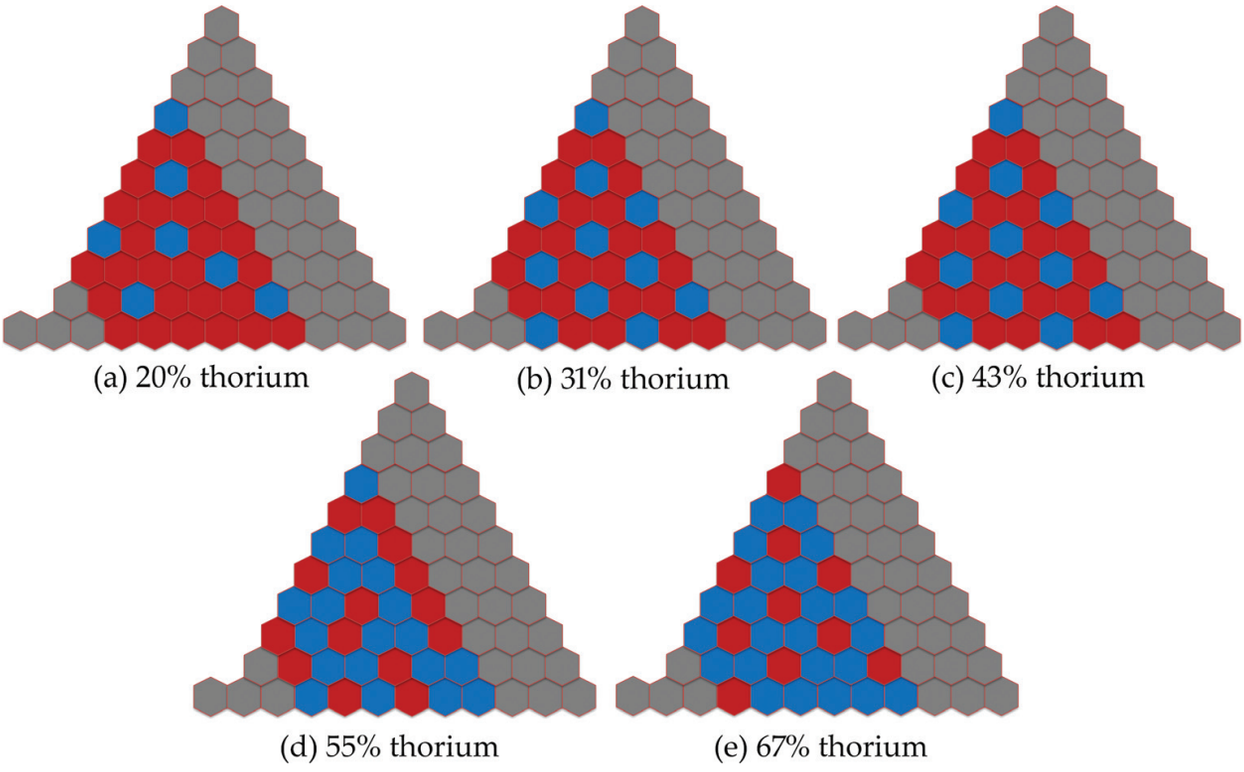


Figure 10. Configurations of thorium/uranium fuel blocks for block-level separation (red: uranium fuel blocks, blue: thorium fuel blocks).

U-238, in the fuel. The mass fraction of fissile isotopes, that is, U-235, is the so-called enrichment of U-235, as defined in Eq. (1).,

$$\varepsilon = \frac{m_{U5}}{m_{U5} + m_{U8}} \tag{1}$$

When another fertile isotope, that is, Th-232, appears in the reactor fuel, the mass fraction of fissile isotopes, as defined in Eq. (2)

$$\varepsilon_{eff} = \frac{m_{U5}}{m_{U5} + m_{U8} + m_{Th2}} \tag{2}$$

is different from the traditional enrichment of U-235, which is called effective enrichment of U-235[19]. If the concept of the effective enrichment of U-235 is adopted, the nominal mass fraction of fissile isotopes is far less than 20% for the thorium-fueled HTRs as shown in **Figure 11**, which is the limit enrichment of U-235 for low-enriched fuel. Since the enrichment of U-235 is no longer equal to the effective enrichment of U-235 in a thorium-loaded reactor, and the physical meaning of the latter is clearer, the latter is analyzed instead of the former.

As shown in **Figure 11**, the required initial effective enrichment of U-235 obviously decreases with the increase of separation level from Th/U MOX to SBU and WASB for the same 2-year

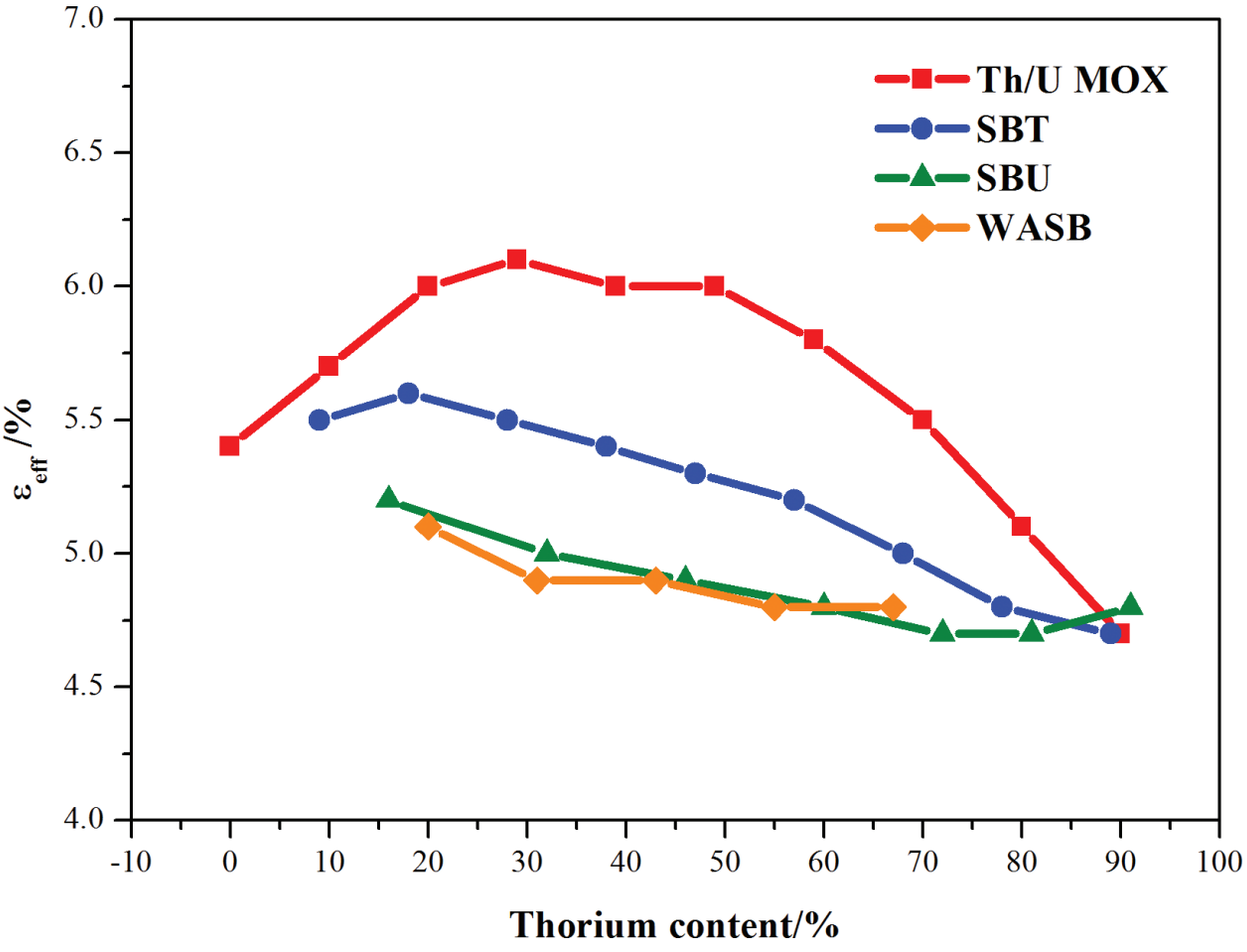


Figure 11. Initial effective enrichment of U-235 as a function of thorium content for different separation levels.

refueling cycle length, when the thorium content changes from 10 to 80%. When the thorium content is less than 10% or larger than 80%, the influence of spatial separation level on the initial ε_{eff} is weak because the fuel is nearly uranium or thorium and thus there is no obvious difference. Moreover, the initial ε_{eff} of SBU is nearly the same as that of theWASB when the thorium content is in the range of 20–70%. For the Th/U MOX fuel, the initial ε_{eff} increases when the thorium content increases from 0 to 30% and decreases with the further increase of thorium. For the SBT, SBU, and WASB, the initial ε_{eff} decreases with the increase of the thorium content.

Although the total initial inventory of heavy metal slightly decreases because of the density difference between ThO_2 (9.4 g/cm^3) and UO_2 (10.4 g/cm^3), as shown in **Figure 12**, the required initial inventory of U-235,as shown in **Figure 13**, nearly has the same trend as the initial effective enrichment of U-235, according to Eq. (2). Furthermore, the initial inventory of the enriched uranium also decreases with the increase of the thorium content, as shown in **Figure 12**, because more and more U-238 is replaced by Th-232 in the reactor core. The change of the initial inventory of U-235 or the initial effective enrichment of U-235 is a result of the difference of nuclear performance (e.g., initial effective multiplication factor and average conversion ratio) caused by the spatial separation levels, as furtherly discussed in Section 3.3.

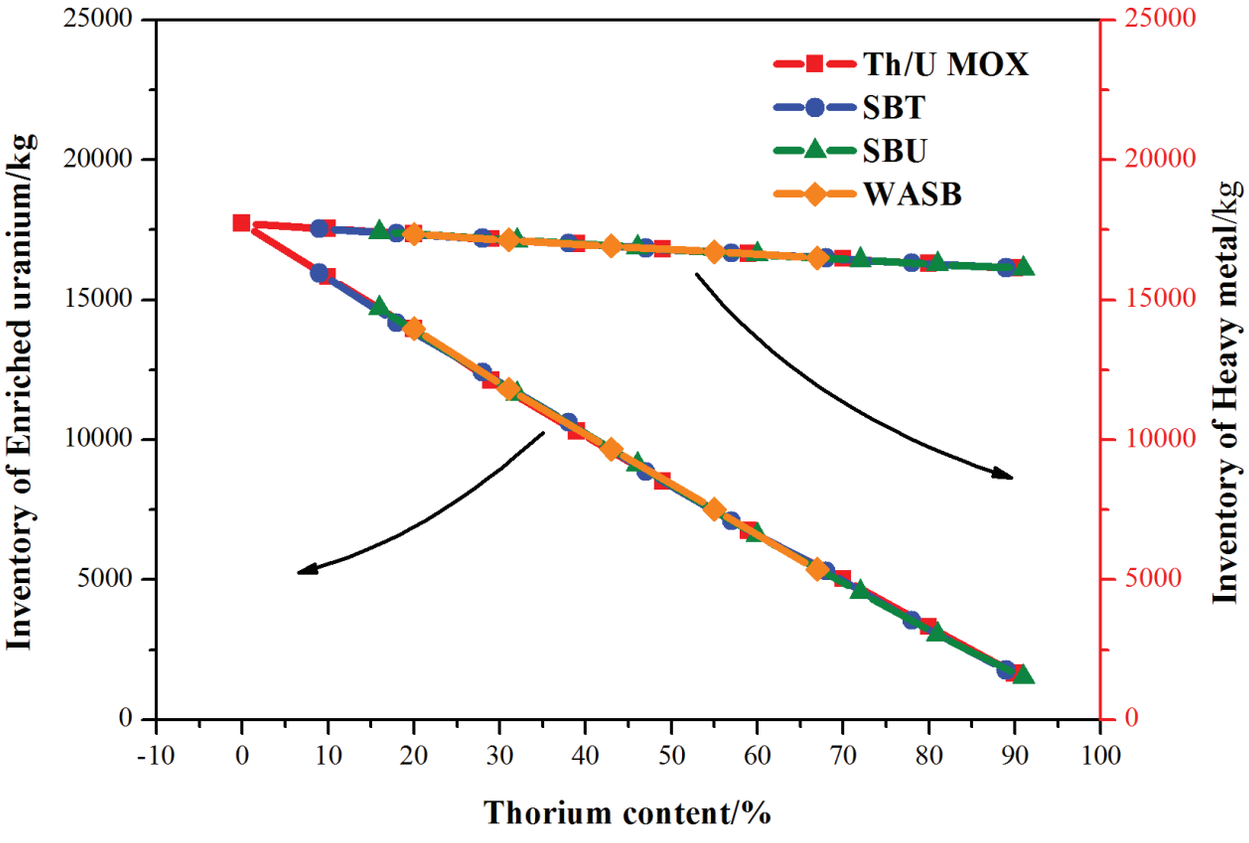


Figure 12. Initial inventory of heavy metal as a function of thorium content for different separation levels.

http://dx.doi.org/10.5772/intechopen.68671

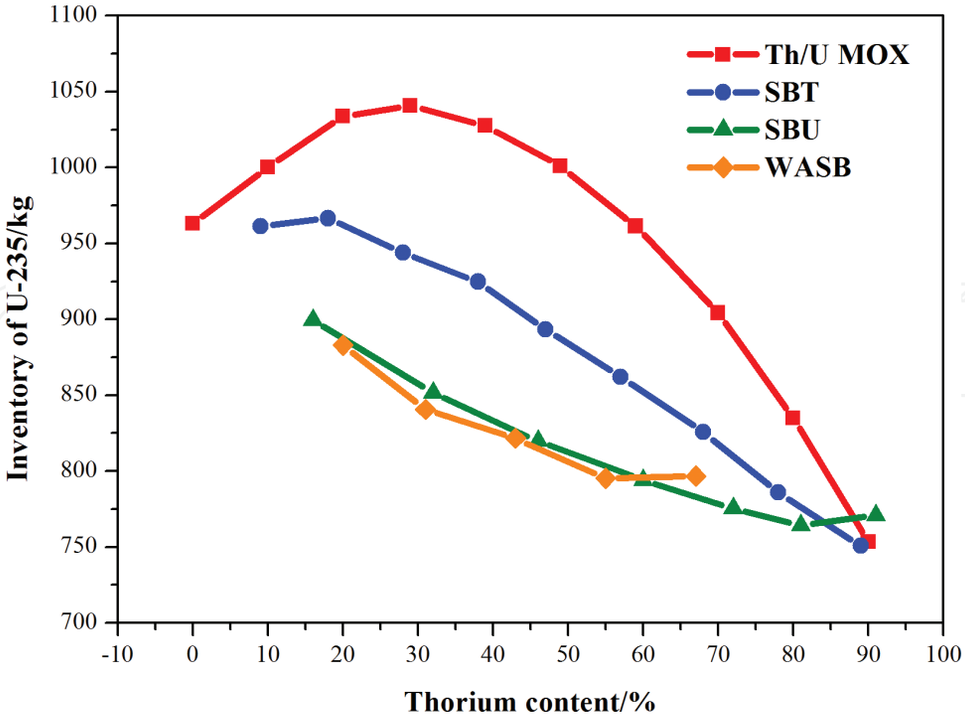


Figure 13. Initial inventory of U-235 as a function of thorium content for different separation levels.

3.3. Initial effective multiplication factor

3.3.1. Initial effective multiplication factor and average conversion ratio

Figure 14 presents the initial effective multiplication factors (k_{eff}) and average conversion ratios (ACRs) of four spatial separation levels as a function of thorium content. For each spatial separation level, the k_{eff} nearly decreases with the increase of thorium content. For the same thorium content, the initial k_{eff} usually increases when the spatial separation level increases

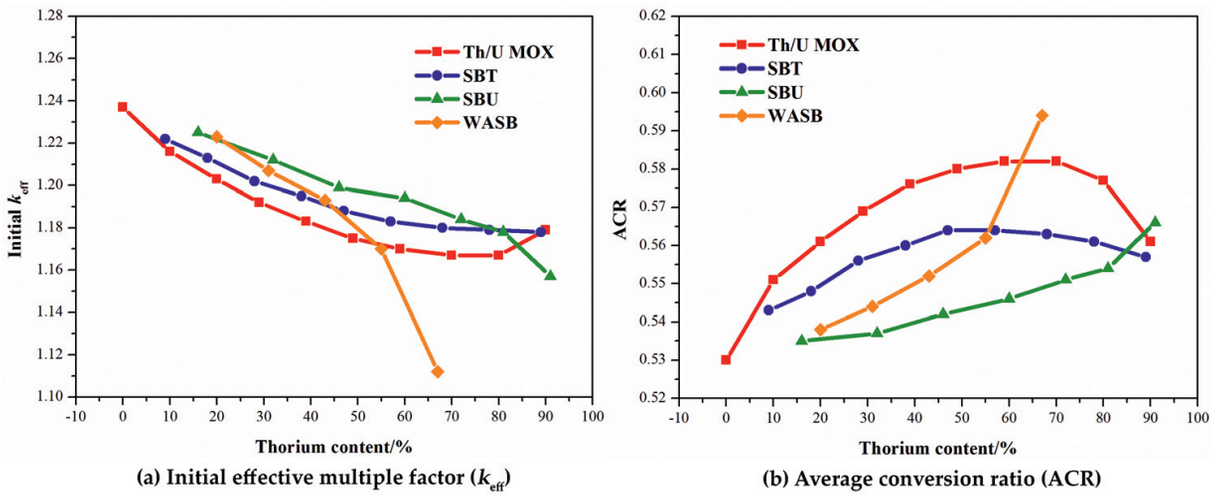


Figure 14. Initial k_{eff} and average conversion ratio of different spatial separation levels.

from Th/U MOX to SBU. When the thorium content is larger than 80%, the difference among them becomes small. The more interesting rule is that the trend of ACR is always opposite to the initial k_{eff}, that is, when the ACR is higher, initial k_{eff} is smaller, even for the WASB level.

Figure 15 presents the k_{eff} as a function of operation time for two different ACRs in one refueling cycle. In these calculations, the refueling cycle length is 657 effective full power days (EFPDs), which means the coordinate of end of cycle (EOC) is fixed, as the point B (657,1.005) in **Figure 15**. On the other hand, the k_{eff} is a nearly linear function of burnup for the thorium-fueled HTR as shown in **Figure 15**. Therefore, if the average conversion ratio of the refueling cycle is smaller, the reactivity drop is larger and thus the initial k_{eff} must be higher to guarantee a critical reactor at EOC.

If **Figure 14** is compared with **Figure 11** or **Figure 13**, it is interesting to find that when the spatial separation level of thorium/uranium fuels changes from SBU to Th/U MOX, the required initial inventory of U-235 is the most for the Th/U MOX in order to achieve the same operation time, but the initial k_{eff} is smallest and the main benefit is the most amount of Th-232 transmuted into U-233. Once the spatial separation of thorium/uranium fuels changes from SBU to WASB, the required initial inventory of U-235 decreases. Moreover, the ACR increases

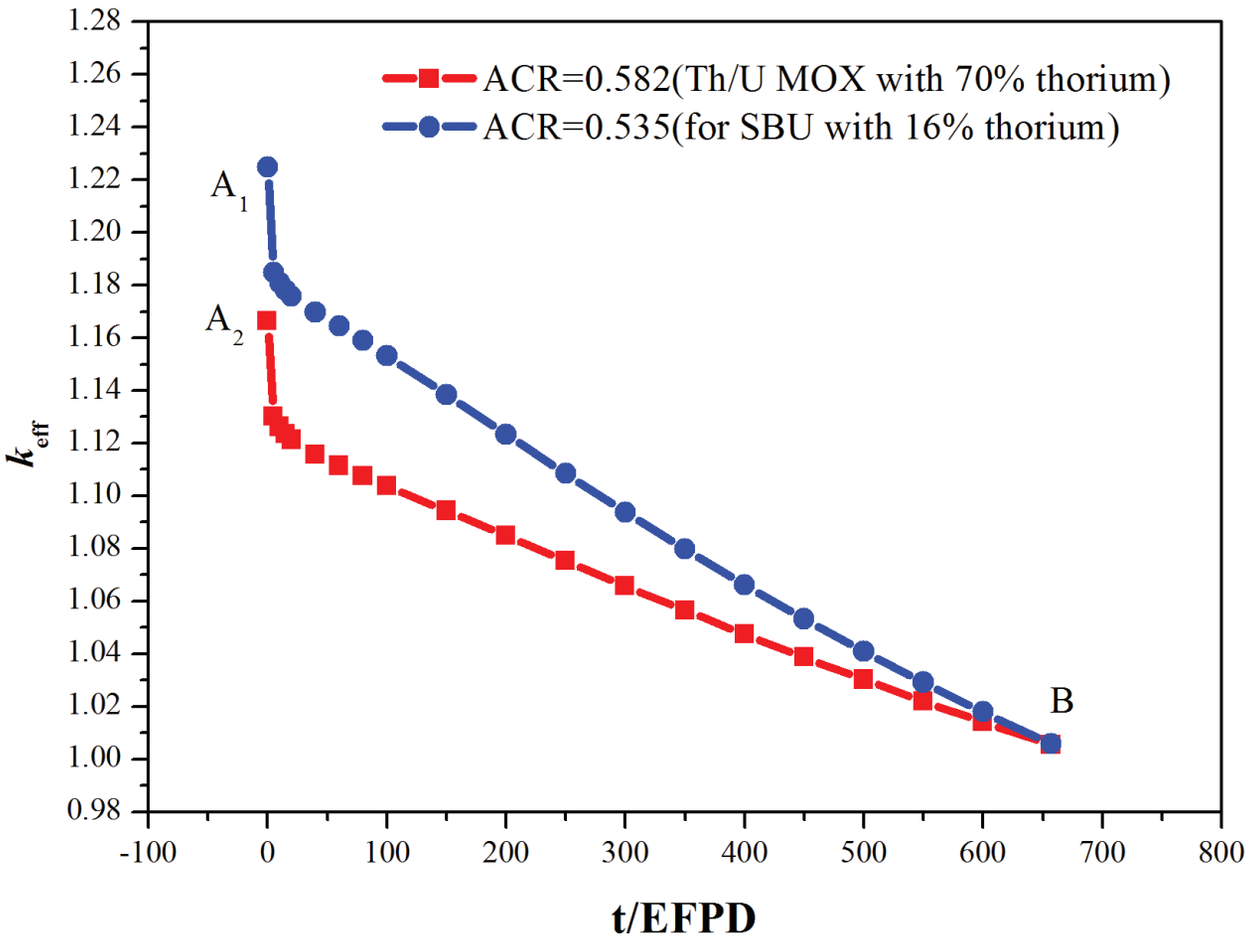


Figure 15. k_{eff} as a function of EFPD for different average conversion ratios.

with increase of thorium content, the initial k_{eff} decreases, and thus the reactivity drop or swingdecreases in the refueling length.

3.3.2. Further discussion of initial effective multiplication factor

In order to analyze the influence of spatial separation levels and thorium content on the initial k_{eff} and thus the initial inventory of U-235, four control groups of typical reactor cores including spatial separation levels and thorium content are calculated and discussed. The group 1 is to compare the Th/U MOX with SBU with 50% thorium content, in order to explain the reason of the decrease of the initial inventory of U-235. The group 2 is to compare the SBU and WASB with 50% thorium content, in order to explain the difference between them. The groups 3 and 4 are to discuss the Th/U MOX with 0, 30, and 80% thorium content, respectively, in order to explain the influence of the thorium content.

Table 4 presents the five factors and initial k_{eff} of the reactor cores involved in the four control groups, which are calculated according to the validated method [10]. The five-factor formula [20] can be written as

$$k_{\text{eff}} = \eta f p \varepsilon P_{\text{NL}} \tag{3}$$

where η, f, p, ε, P_{NL} are, respectively, the reproduction factor, fuel utilization factor, resonance escape probability, fast fission factor, and nonleakage probability. However, in the core physics calculation described in Section 2.2.1, the homogenization of fuel block will mix the fuel, moderator, and coolant into a mixture, making the η and f inseparable. Thus, the production of η and f is regarded as the reproduction factor of the core. More information about the five-factor formula can be found in Ref. [10].

To quantitatively describe the contribution of each factor to the variation of the initial effective multiplication factor, its contribution [21] is defined in terms of the components of five-factor formula

$$\Delta r = \left(\frac{1}{\frac{r_1}{\bar{r}} \cdot \bar{k}} - \frac{1}{\frac{r_2}{\bar{r}} \cdot \bar{k}} \right) \cdot 10^5, \qquad r = \eta f, \varepsilon, p, P_{\text{NL}} \tag{4}$$

Reactor core	ηf	ε	p	P_{NL}	k_{eff}
Th/U MOX-0%Th	1.7257	1.0804	0.6994	0.9550	1.24531
Th/U MOX-30%Th	1.6891	1.0861	0.6852	0.9551	1.20058
Th/U MOX-80%Th	1.5540	1.0701	0.7379	0.9570	1.17436
Th/U MOX-50%Th	1.6491	1.0830	0.6935	0.9556	1.18358
SBU-50%Th	1.5690	1.0687	0.7508	0.9567	1.20442
WASB-50%Th	1.5182	1.0734	0.7567	0.9615	1.18567

Table 4. Five factors and initial k_{eff} of different reactor cores involved in four control groups.

where

$$\overline{r} = 0.5(r_1 + r_2), \quad \overline{k} = \overline{\eta f}\,\overline{\varepsilon}\,\overline{p}\,\overline{P_{\mathrm{NL}}} \tag{5}$$

The subscripts 1 and 2 represent two different cases, respectively. **Table 5** presents the contribution of each factor for the four control groups.

For the group 1, when the thorium content is 50% and spatial separation level changes from Th/U MOX level to SBU level, the nonleakage probability increases by 96 pcm and contributes +6% to the initial k_{eff}, because the spatial separation level strengthens thorium absorption, and the microscopic absorption cross section of Th-232 (7.4 barns) is three times of U-238 (2.7 barns). Based on the same reason, more thermal neutrons are absorbed by Th-232 but cannot induce fission reactions, which leads to the reproduction factor of core (ηf) to decrease by 4167 pcm and contributes −285% to the initial k_{eff}. The fast fission cross-section of Th-232 (0.01 barns) is smaller than that of U-238 (0.04 barns), which causes the fast fission factor (ε) to decrease by 1112 pcm and contribute −76%. However, because the thorium fuel is lumped in the thorium compacts for the SBU-50%Th and a smaller resonance integral (RI) of Th-232 (85) compared to U-238's (275), the resonance escape probability (p) of the SBU-50%Th increases by 6649 pcm and contributes +455%. As a result of all effects, especially the contribution of the increase of p, the initial k_{eff} of the SBU-50%Th is 1460 pcm larger than that of the Th/U MOX-50%Th. The spatial self-shielding effect is strengthened by Th-232 and spatial separation levels, and thus the increase of resonance escape probability leads to the decrease of 188 kg initial inventory of U-235.

For the group 2, when the spatial separation increases from SBU level to WASB level, although the resonance escape probability further increases by 655 pcm, the reproduction factor decreases by 2754 pcm because of the further lumping of the thorium fuel. As a result, the initial k_{eff} decreases by 1313 pcm causing a smaller reactivity swing in the refueling period. Moreover, the initial inventory of U-235 decreases 6 kg because of a larger ACR.

For the group 3, for a fixed spatial separation level, for example, Th/U MOX level, when the thorium content increases from 0 to 30%, more thermal neutrons generated by fission are absorbed by fertile Th-232 because of three-time microscopic absorption cross section of

Group number	Group	$\Delta\eta f$ [pcm]	$\Delta\varepsilon$ [pcm]	Δp [pcm]	ΔP_{NL} [pcm]	Δk_{eff} [pcm]
1	MOX-50%Th	−4167	−1112	+6649	+96	+1460
	SBU-50%Th	(−285%)	(−76%)	(+455%)	(+6%)	(+100%)
2	SBU-50%Th	−2754	+367	+655	+419	−1313
	WASB-50%Th	(−210%)	(+28%)	(+50%)	(+32%)	(−100%)
3	MOX-0%Th	−1753	+430	−1677	+9	−2992
	MOX-30%Th	(−59%)	(+14%)	(−56%)	(+1%)	(−100%)
4	MOX-30%Th	−7017	−1250	+6236	+171	−1857
	MOX-80%Th	(−378%)	(−67%)	(+336%)	(+9%)	(−100%)

Table 5. Contribution of each factor to variation of initial k_{eff}.

http://dx.doi.org/10.5772/intechopen.68671

Th-232, which leads to the decrease of the reproduction factor by 1753 pcm. Moreover, because of harder neutron spectrum, the resonance escape probability decreases by 1677 pcm. As a result, the initial k_{eff} decreases by 2992 pcm and the required initial inventory of U-235 increases by 77.8 kg. If the thorium content further increases from 30 to 80%, as shown in the group 4, a large amount of U-238 is replaced by Th-232 in the reactor core. Because of a smaller resonance integral of Th-232 (85) compared to U-238's (275), the resonance escape probability (p) increases by 6236 pcm and contributes +336% but the reproduction factor decreases by 7017 pcm and contributes −378%. As a result, the initial k_{eff} decreases by 1857 pcm. Moreover, the required initial inventory of U-235 decreases by 206 kg because of a larger ACR.

3.4. Fuel cycle cost analysis

Using the levelized lifetime cost methodology described in Section 2.2.2, the fuel cycle cost of the four types of reactor cores (Th/U MOX, SBT, SBU, and WASB) analyzed in Sections 3.2 and 3.3 as a function of thorium content is shown in **Figure 16**. Compared with **Figures 11** or **13**, the fuel cycle cost changes with the same trend as the effective enrichment of U-235 or the initial inventory of U-235 in the reactor cores. When the thorium content is constant, the fuel cycle cost decreases with the increase of the spatial separation level. However, the difference of the SBU level and WASB level is small. The fuel cycle cost decreases with the increase of the

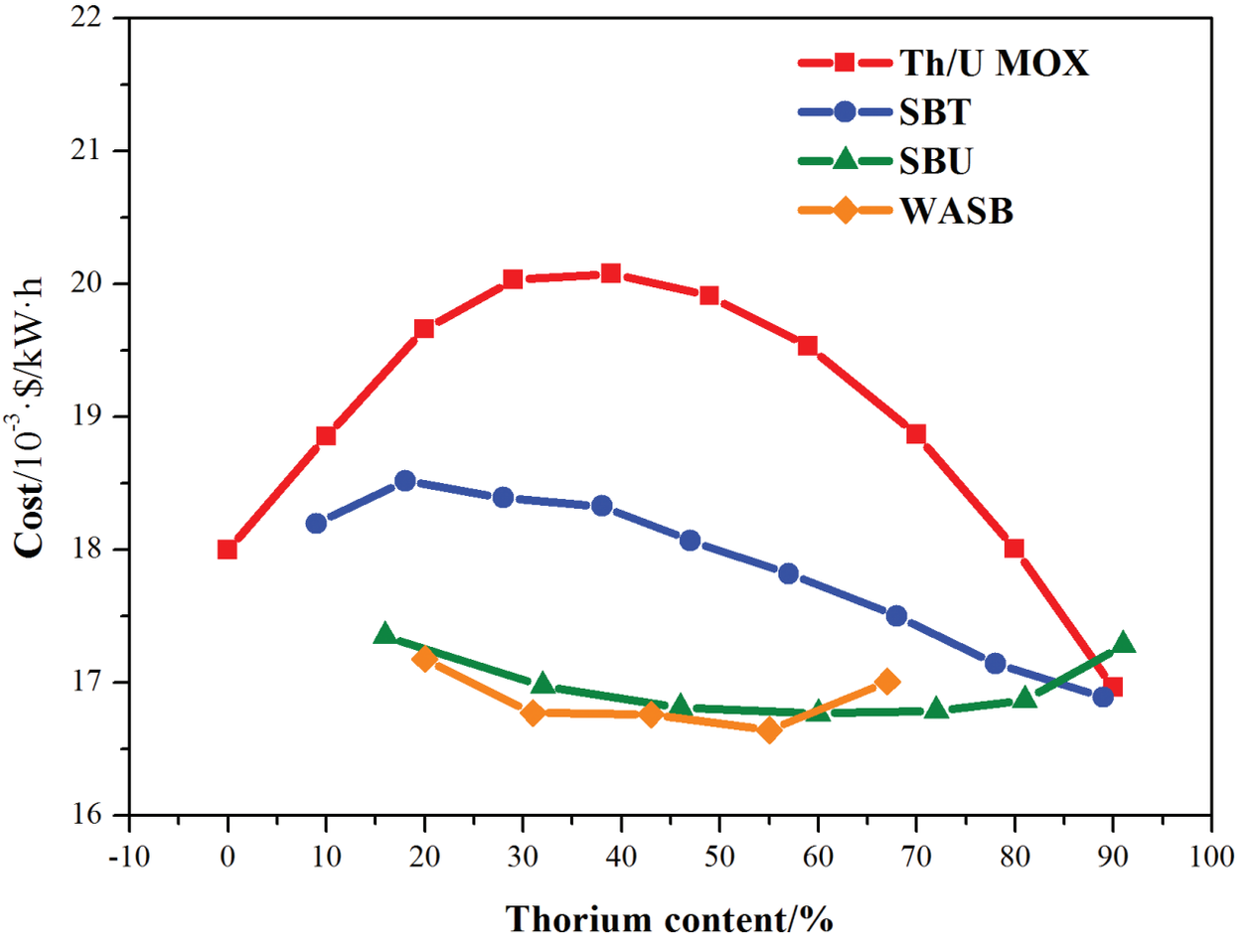


Figure 16. Fuel cycle cost of different spatial separation levels.

thorium content for the SBT, SBU, and WASB levels. However, it increases in the range of thorium content from 0 to 40% and decreases when the thorium content is larger than 40%.

The tight relationship between fuel cycle cost and initial inventory of U-235 mainly results from the composition of the cost. **Figure 17** presents the composition of fuel cycle cost for three different reactor cores, including natural uranium purchase, thorium purchase, uranium conversion, uranium enrichment, the fabrication of fuel blocks, and storage and the deposal of spent fuels. Because the required amount of natural uranium is 13 times of the inventory of heavy metal in the reactor core due to 0.7% U-235 in natural uranium, both the natural uranium purchase and uranium enrichment are 70% of total fuel cycle cost. The thorium purchase is only 2.5% because the thorium need not be enriched, and the required amount of thorium is by far less than the amount of the natural uranium. The fabrication cost is the highest unit price (777 $/kg HM) and the fabrication involves all heavy metals, so it is about 20% of the total cost. Although the unit price of the disposal of spent fuel is also high (610 $/kg HM), the disposal cost is only about 0.5% because of so-called time value.

The fuel cycle cost is mainly determined by natural uranium purchase (35–40%), uranium enrichment (32–35%), and the fabrication of fuel blocks (18–21%). The total of three items is 85–96% fuel cost. The fabrication cost is the same for all reactor cores because the inventory of heavy metal in the reactor core is the same. The natural uranium purchase and uranium enrichment are directly related to the initial inventory of U-235. The more is the inventory of U-235, the more are the required natural uranium and the uranium enrichment. As a result, the fuel cycle cost is the same trend as the initial inventory of U-235 or the initial effective enrichment.

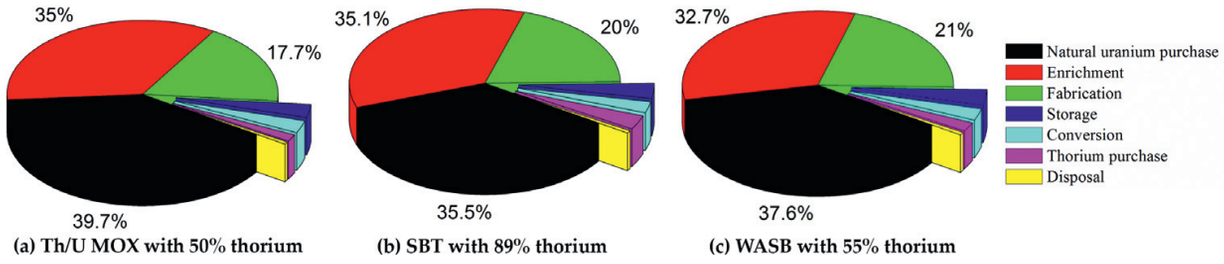


Figure 17. Composition of fuel cycle cost for some typical reactor cores.

4. Conclusions

In order to utilize thorium fuel in block-type HTRs with the features of inherent passive safety, high burnup, and hard neutron spectrum, two key factors of thorium content and spatial separation levels are chosen to be investigated. The thorium content represents the thorium/uranium fuel composition and the spatial separation level represents the spatial distribution of thorium/uranium fuels. For every thorium content,the spatial distribution of thorium and uranium fuels are concluded into four spatial separation levels, that is, no separation level (Th/U MOX), TRISO level (SBT), channel level (SBU), and block level (WASB) for the thorium-fueled block-type HTRs.

The nuclear performance of the reactor core, that is, initial effective multiplication factor, average conversion ratio, and initial inventory of U-235, under four spatial separation levels are obtained in the one-batch fixed-pattern refueling mode by the two-step calculation scheme developed based on the DRAGON. For every thorium content, the initial inventory of U-235 decreases with the increase of the spatial separation level from Th/U MOX to WASB, because spatial self-shielding effect is strengthened by the lumped thorium and uranium. However, the SBU level is nearly the same as the WASB level. If the multiple fuel batches and realistic refueling patterns are considered, the difference of the SBU from the WASB could be large. On the other hand, the initial inventory of U-235 decreases with the increase of the thorium content for the SBT, SBU, and WASB levels. However, for Th/U MOX level, it increases in the range of thorium content from 0 to 30% and decreases when it is larger than 30% because of the better performance of U-233 than Pu-239 in thermal reactors.

The performance difference of the four spatial separation levels is synthetically evaluated bythe levelized lifetime cost method.The fuel cycle cost of the Th/U MOX, SBT, SBU, and WASB changes with the same trend as the effective enrichment of U-235 or the initial inventory of U-235 in the reactor cores because the latter determines 70% of the total cost.

Acknowledgements

This work is supported by the National Natural Science Foundation of China (11405036).

Author details

Ming Ding[1]* and Jie Huang[1,2]

*Address all correspondence to: dingming@hrbeu.edu.cn

1 Harbin Engineering University, Harbin, China

2 China Nuclear Power Technology Research Institute, Shenzhen, China

References

[1] Baumer R, Barnert H, Baust E, Bergerfurth A, et al. AVR: Experimental High Temperature Reactor, 21 Years of Successful Operation for a Future Energy Technology. Dusseldorf: VDI-Verlag GmbH; 1990. p. 379

[2] Habush AL, Harris AM. 330-MW(e) fort St. Vrain high-temperature gascooled reactor. Nuclear Engineering and Design. 1968;**7**(4):312–321. DOI: 10.1016/0029-5493(68)90064-2

[3] Lung M, Gremm O. Perspectives of the thorium fuel cycle. Nuclear Engineering and Design. 1998;**180**(2):133–146. DOI: 10.1016/S0029-5493(97)00296-3

[4] International Atomic Energy Agency. Thorium Fuel Cycle-Potential Benefits and Challenges. Vienna: International Atomic Energy Agency; 2005. p 105

[5] Wang D. Optimization of a seed and blanket thorium-uranium fuel cycle for pressurized water reactors [thesis]. Cambridge: Massachusetts Institute of Technology; 2003.

[6] Shwageraus E, Zhao XF, Diriscoll MJ, Hejzlar P, Kazimi MS. Microhetero-geneous thoria-urania fuels for pressurized water reactors. Nuclear Technology. 2004;**147**,20–36

[7] Olson G, McCardell R, Illum D. Fuel summary report: shippingport lightwater breeder reactor (Technical report). INEEL/EXT-98-00799. Idaho Fall: Idaho National Engineering and Environmental Laboratory; 1999

[8] Radkowsky A, Galperin A. The nonproliferative light water thorium reactora new approach to light water reactor core technology. Nuclear Technology. 1998;**124**,215–222

[9] Ding M, Kloosterman JL. Thorium utilization in a small long-life HTR. Part II: Seed-and-blanket fuel blocks. Nuclear Engineering and Design. 2014;**267**,245–252

[10] Jie Huang, Ming Ding. Analysis of multi-scale spatial separation in a block-type thorium-loaded helium-cooled high-temperature reactor. Annals of Nuclear Energy. 2017;**101**:89–98

[11] Jie Huang, Ming Ding. Analysis of thorium content and spatial separation influence for seed and blanket fuel blocks in the AHTR. Progress in Nuclear Energy. 2016;**90**:182–189

[12] GA. Gas turbine-modular helium reactor (GT-MHR) conceptual design description report (Technical report). 910720. California: General Atomics; 1996

[13] Hébert A.. Toward DRAGON Version 4. In: Topical Meeting on Reactor Physics: Advances in Nuclear Analysis and Simulation (PHYSOR-2006). 10–14 September; Vancouver, Canada

[14] Hébert A. Collision Probability Analysis of the Double-Heterogeneity Problem. Nuclear Science and Engineering. 1993;**115**:177

[15] Sanchez R. Renormalized treatment of the double heterogeneity with the method of characteristics. In: Int. Mtg. on the Physics of Fuel Cycles and Advanced Nuclear Systems: Global Developments (PHYSOR-2004); 25–29 April 2004; Chicago, Illinois

[16] OECD. The Economics of the Nuclear Fuel Cycle (Technical report). Paris: Organization for Economic Co-operation and Development; 1994

[17] Holcomb DE, Peretz FJ, Qualls AL. Advanced high temperature reactor systems and economic analysis (Technical report). ORNL/TM-2011/364. Oak Ridge: Oak Ridge National Laboratory; 2011

[18] Jie H, Ming D, Yongyong Y. Fuel cycle cost analysis of Th/U MOX fuel in a block-type HTR. In: 8th International Topical Meeting on High Temperature Reactor Technology (HTR-2016); 6–10 November 2016; Las Vegas, USA

[19] Verrue J, Ding M, Kloosterman JL. Thorium utilisation in a small long-life HTR. Part III: Composite-compact fuel blocks. Nuclear Engineering and Design. 2014;**267**,253–262

[20] Duderstadt JJ, Hamilton LJ. Nuclear Reactor Analysis. New York: John Wiley & Sons, Inc.; 1976. pp. 295–299

[21] ORNL. Status of the physics and safety analyses for the liquid-salt-cooled very high-temperature (Technical report). ORNL/TM-2005/218. Oak Ridge: Oak Ridge National Laboratory; 2005

IntechOpen

IntechOpen

IntechOpen

IntechOpen